

2006-09-01

Chirality dependence of the radial breathing phonon mode density in single wall carbon nanotubes

AN Vamivakas, Y Yin, AG Walsh, MS Unlu, BB Goldberg, AK Swan. 2006. "Chirality dependence of the radial breathing phonon mode density in single wall carbon nanotubes."

<https://hdl.handle.net/2144/31461>

Downloaded from DSpace Repository, DSpace Institution's institutional repository

Chirality dependence of the radial breathing phonon mode density in single wall carbon nanotubes

A. N. Vamivakas^{1,*}, Y. Yin², A. G. Walsh², M. S. Ünlü¹, B. B. Goldberg², and A. K. Swan¹

¹*Department of Electrical and Computer Engineering,*

Boston University, 8 St. Mary's St.,

Boston, Massachusetts 02215, USA

²*Department of Physics, Boston University,*

590 Commonwealth Ave., Boston, Massachusetts 02215

(Dated: May 1, 2017)

Abstract

A mass and spring model is used to calculate the phonon mode dispersion for single wall carbon nanotubes (SWNTs) of arbitrary chirality. The calculated dispersions are used to determine the chirality dependence of the radial breathing phonon mode (RBM) density. Van Hove singularities, usually discussed in the context of the single particle electronic excitation spectrum, are found in the RBM density of states with distinct qualitative differences for zig zag, armchair and chiral SWNTs. The influence the phonon mode density has on the two phonon resonant Raman scattering cross-section is discussed.

PACS numbers: 81.07.De,63.22.+m

Understanding how spatial confinement influences both a material's excitation spectrum and the density of excitation modes is imperative to accurately modeling the observable properties of the system. In particular, there has been much recent interest in the nanoscale confinement of phonons¹. In one-dimensional (1D) single wall carbon nanotubes (SWNTs), there are various methods employed to calculate the phonon mode dispersion. Early work, following the successful calculations of the single electron bandstructure, projected the two-dimensional (2D) graphene phonon dispersion relation to 1D. It was quickly realized, though, that zone-folding did not capture all the phonon modes of SWNTs². Following some *ab-initio* work^{3,4}, a microscopic mass and spring model has been formulated^{5,6} to accurately capture the lattice dynamical properties of SWNTs. The mass and spring model permits calculation of both the phonon dispersion relation and phonon mode density for SWNTs of arbitrary chirality.

In the optical characterization of SWNTs, one phonon resonant Raman scattering (1phRRS) is employed to measure a tube's electronic resonances, investigate various Raman active phonon modes and even determine the physical diameter and chirality of the tube under study². Though 1phRRS is a powerful tool for SWNTs characterization, conservation of momentum allows only a single phonon to contribute to the measured signal at a particular scattered photon frequency. In contrast, in two phonon Raman scattering, multiple phonon pairs originating from the full phonon dispersion curve can contribute to the scattered signal. Therefore, the two phonon resonant Raman scattering (2phRRS) cross-section, unlike the 1phRRS case, is proportional to the phonon joint density of states (DOS). The 2phRRS cross-section is nonzero for all scattered frequencies for which the product of the phonon joint DOS and transition matrix element is nonzero. Although 2phRRS has been discussed in the context of SWNTs, the discussion has only focused on calculating $|W_{i \rightarrow f}^{2-ph}|^2$ and little attention has been paid to the density of phonon modes². It is clear then, in 2phRRS, an accurate model of both the phonon dispersion and joint DOS is important.

To calculate the phonon dispersion and DOS we model the nanotube lattice as a collection of equal mass points, capable of displacing in all three spatial dimensions. We use Newton's law $\vec{F} = -k\vec{x} = m\ddot{\vec{a}}$ to understand the dynamical evolution of each lattice site^{5,6}. The governing equation is

$$\Omega^2 \vec{Q} = \underline{W}(\alpha, q; n, m) \vec{Q} \quad (1)$$

where (n, m) index the nanotube, $\alpha = 0, 1, \dots, N - 1$, $N = \frac{2(n^2+m^2+nm)}{\gcd(2n+m, 2m+n)}$ equals the number of graphene unit cells in the nanotube unit cell, q is the 1D phonon crystal momentum along the tube axis, $\Omega^2 = m\omega^2/K_1$ is the rescaled phonon mode frequency where K_1 is the force constant that characterizes the strength of the various couplings to be described below, $\vec{Q} = [Q_{A,\rho} \ Q_{A,\theta} \ Q_{A,z} \ Q_{B,\rho} \ Q_{B,\theta} \ Q_{B,z}]$ is the vector of fourier amplitudes for lattice site displacements with $Q_{i,j}$ indicating the carbon atom at basis site i displaces in the direction j and the matrix dictating the dynamics is

$$\underline{W} = \left(s_1 M_{1stNN} + s_2 M_{2ndNN} + s_3 M_{rbb} \right). \quad (2)$$

In \underline{W} , M_{1stNN} is a 6x6 matrix characterizing the influence first nearest neighbor carbons atoms have in displacing a specific basis atom, M_{2ndNN} is a 6x6 matrix characterizing the influence second nearest neighbor carbon atoms have in displacing a specific basis atom and M_{rbb} is a 6x6 matrix characterizing the restoring force on a given basis site resulting from bending the bond between neighboring carbon atoms. The above dynamics allow each carbon atom to displace in the ρ , θ , and z directions. In Eq. (2), s_i determines the relative strength of the given coupling with respect to the coupling characterized by the spring constant K_1 . Specifically, $s_i = \frac{K_i}{K_1}$ where K_i is the spring constant characterizing the i^{th} restoring force. The parameter α serves as a band index for the phonons, where the number of phonon bands for a given nanotube is equal to three times the number of carbon atoms in the nanotube unit cell. For fixed α , the phonon mode dispersion relation is calculated by diagonalizing Eq. (2) as a function of q as q ranges throughout the nanotube's first Brillouin zone.

In addition to determining the dispersion relation, it is also possible to calculate the 1D phonon density of states. Generally, the density of phonon modes is an important quantity when calculating transition rates for scattering processes mediated by phonons. We are particularly interested in the two phonon Raman scattering process. The two phonon mediated Raman scattering cross-section, assuming free electrons and holes, is⁷

$$\frac{d\sigma_{RRS}^{2-ph}}{d\Omega d\omega_s} = C \rho_{DOS}^{(2-ph)}(2\Omega_p) \cdot |W_{i \rightarrow f}^{2-ph}(\omega_l, \vec{e}_l; \omega_s = \omega_l - 2\Omega_p, \vec{e}_s)|^2 \quad (3)$$

where we have assumed Stokes scattering, C is a constant, $\rho_{DOS}^{(2-ph)}(2\Omega_p)$ is the two phonon density of states and $|W_{i \rightarrow f}^{2-ph}|^2$ is the transition probability from initial system state i , with

a single pump photon, to a final state f , with a single scattered photon and a pair of degenerate single phonons with opposite crystal momentum. We note, in Eq. (3) our focus is on final states that contain two degenerate phonons of frequency Ω_p . In 2phRRS, it is also possible to have scattered photons at $\omega_s = \omega_l - (\Omega_{p1} \pm \Omega_{p2})$, the sum or difference frequency of two nondegenerate phonons. In a 1-dimensional system, our expectation is the reduction of phonon phase space will hamper the likelihood of simultaneously satisfying both energy and momentum conservation in the sum or difference frequency generation process so we have ignored this possibility in Eq. (3).

The utility in focusing on the degenerate phonon generation, is that we can approximate $\rho_{DOS}^{(2-ph)}(2\Omega_p)$ by $\rho_{DOS}^{(1-ph)}(\Omega_p)$ ⁷. With the single particle density of states defined as⁸

$$\rho_{DOS}(\Omega)d\Omega \propto \frac{1}{\left|\frac{d\Omega}{dq}\right|}d\Omega \quad (4)$$

we can evaluate $\rho_{DOS}^{(1-ph)}(\Omega_p)$ for a given phonon band with knowledge of $\Omega_p(q; \alpha)$. In degenerate 2phRRS, $\rho_{DOS}^{(1-ph)}(\Omega_p)$ serves as an indicator of how many phonon pairs contribute to a specific scattered photon frequency. Specifically, the regions of zero slope in the phonon dispersion result in Van Hove singularities⁹ that enhance the 2phRRS cross-section.

To illustrate the chirality dependence of the RBM single phonon density of states, we study nanotube families $2n + m = 22$ and $2n + m = 23$ as well as subsets of both armchair and zig zag tubes. Our interest in family 22 stems from recent experimental work in 2phRRS from single SWNTs¹⁰. In addition, family 22 and 23 yields a set of semiconducting SWNTs with chiral angles ranging from 0° to 30° .

Before studying the radial breathing mode (RBM) DOS, we illustrate a typical phonon dispersion relation calculated from Eq. (2). Figure 1(a) is the full phonon dispersion relation for an (11,0) nanotube (family 22). The number of carbon atoms in the nanotube unit cell is 44 which results in $3 * 44 = 132$ phonon modes. Also, the length of the primitive lattice vector along the tube axis is 3 times the carbon-carbon distance on the graphene lattice. To fix the frequency axis, we have followed Mahan⁵ and set $\Omega = \sqrt{3}$ equal to $\omega = 1600 \text{ cm}^{-1}$ (this fixes the value of the free parameter K_1). We also assumed in Eq. (2) that $s_1 = 1$, $s_2 = 0.06$ and $s_3 = 0.024$ ⁵. The calculated zone center frequency for the RBM of the (11,0) tube is 266 cm^{-1} . The calculated value is in near perfect agreement with recently reported RBM-diameter relation of $\omega_{RBM} = \frac{215}{D} + 18$ where D is the nanotube diameter¹¹, which

yields a zone center RBM frequency of 267.4 cm^{-1} for the (11,0) nanotube.

Now we investigate the RBM DOS chirality dependence. In Fig. 1(b), we plot the RBM dispersion curve and RBM DOS for SWNTs of family 22. With the exception of the tube (11,0), which will be discussed when we focus on the zig zag tubes, the other tubes comprising family 22 have RBMs with mode densities concentrated entirely at the zone center. In addition, the chiral tubes of family 22 have RBMs that exhibit very low dispersion across the nanotube Brillouin zone. The Van Hove singularity in the RBM mode density of family 22's chiral tubes results in a 2phRRS cross-section that is entirely mediated by the zone center RBM. In this case, even though the momentum conservation has been relaxed in the two phonon scattering process, the phonon mode density prohibits phonons of appreciable crystal momentum from contributing to the 2phRRS cross-section. Family 23 exhibits qualitatively identical behaviour to family 22.

Figure 2 contains plots of the RBM dispersion, and its associated DOS, for semiconducting zig zag tubes (8,0), (10,0), (11,0) and (13,0) where we note that the RBM bandwidth decreases with decreasing tube diameter. There are two striking features in Fig. 2(a) when compared to the chiral tubes of family 22. First, the bandwidth of the RBM is considerably larger than the chiral tubes, nearly 2 orders of magnitude in some cases. Second, zig zag tubes exhibit two sharp Van Hove singularities in their RBM mode density. If we define the zone boundary of the Brillouin zone as q_{max} , we find that only wavevectors out to $0.03 * q_{max}$ contribute to the zone center singularity. In 2phRRS, when the incoming laser frequency is commensurate with an electronic resonance, the two singularities in the RBM mode density should result in two peaks in the scattering cross-section, with a higher intensity peak associated with a frequency that is twice the zone center RBM frequency.

Finally, we examine the RBM dispersion and DOS, plotted in Fig. 2(b), for the (metallic) armchair tubes (7,7), (8,8), (9,9) and (10,10). In comparison to the previous zig zag tubes, the strongest Van Hove singularity for the RBM has shifted from zone center to the vicinity of the zone boundary. Approximately $0.01 * q_{max}$ wavevectors contribute to the zone boundary singularity. The previous observation has an important consequence in 2phRRS. Not only will we observe a double peak in the scattering cross-section when the incoming laser frequency is tuned to an electronic resonance, but the more intense peak will be associated with a frequency that is equal to twice the zone boundary RBM phonon frequency.

In summary, we have used a microscopic model of the lattice dynamical properties of

SWNTs to determine the chirality dependence of the RBM mode density. The importance of the phonon mode density for 2phRRS was discussed and illustrated. For chiral tubes of family 22 and 23 (with the exception of the (11,0) tube), we found narrow band RBMs with Van Hove singularities restricted to the zone center. In 2phRRS, we expect to see spectral features at scattered frequencies that are exactly 2 times the zone center RBM phonon frequency as determined by 1phRRS.

In contrast to the chiral tubes, the set of achiral SWNTs studied exhibited large bandwidth RBMs with 2 Van Hove singularities in their DOS. The zone center Van Hove singularity dominated for zig zag tubes, whereas the zone boundary singularity dominated for armchair SWNTs. The appearance of two Van Hove singularities in achiral tube's mode density allows for the possibility of a 2 peak structure in the 2phRRS cross-section at fixed laser frequency.

Acknowledgments

This work was supported by Air Force Office of Scientific Research under Grant No. MURI F-49620-03-1-0379, by NSF under Grant No. NIRT ECS-0210752 and a Boston University SPRInG grant. The authors would like to thank Gun Sang Jeon for discussions on his microscopic model of achiral nanotube phonons⁵.

* Electronic address: nvami@bu.edu

¹ M. A. Stroschio and M. Dutta, *Phonons in Nanostructures* (Cambridge University Press, 2005).

² S. Reich, C. Thomsen, and J. Maultzsch, *Carbon Nanotubes* (Wiley, VCH, 2004).

³ D. Sánchez-Portal, E. Artacho, J. M. Soler, A. Rubio, and P. Ordejón, *Phys. Rev. B* **59**, 12678 (1999).

⁴ J. Maultzsch, S. Reich, C. Thomsen, E. Dobardžić, I. Milošević, and M. Damnjanović, *Solid State Commun.* **121**, 471 (2002).

⁵ G. D. Mahan and G. S. Jeon, *Phys. Rev. B* **70**, 075405 (2004).

⁶ W. Mu, A. N. Vamivakas, and Z. can Ou-Yang, *to be submitted* *Phys. Rev. B*.

⁷ M. Cardona and G. Güntherodt, eds., *Light Scattering in Solids II* (Springer, Heidelberg, 1982),

vol. 50 of *Topics in Applied Physics*, chap. 2, p. 19.

⁸ C. Kittel, *Introduction to Solid State Physics* (Wiley, 1995), seventh edition ed.

⁹ L. V. Hove, *Phys. Rev.* **89**, 1189 (1953).

¹⁰ Y. Yin, S. Cronin, A. Walsh, A. Stolyarov, M. Tinkham, A. N. Vamivakas, W. Basca, M. S. Ünlü, B. B. Goldberg, and A. K. Swan, accepted for publication in *IEEE J. Sel. Top. Quantum Electron.*.

¹¹ J. Maultzsch, H. Telg, S. Reich, and C. Thomsen, *Phys. Rev. B* **72**, 205438 (2005).

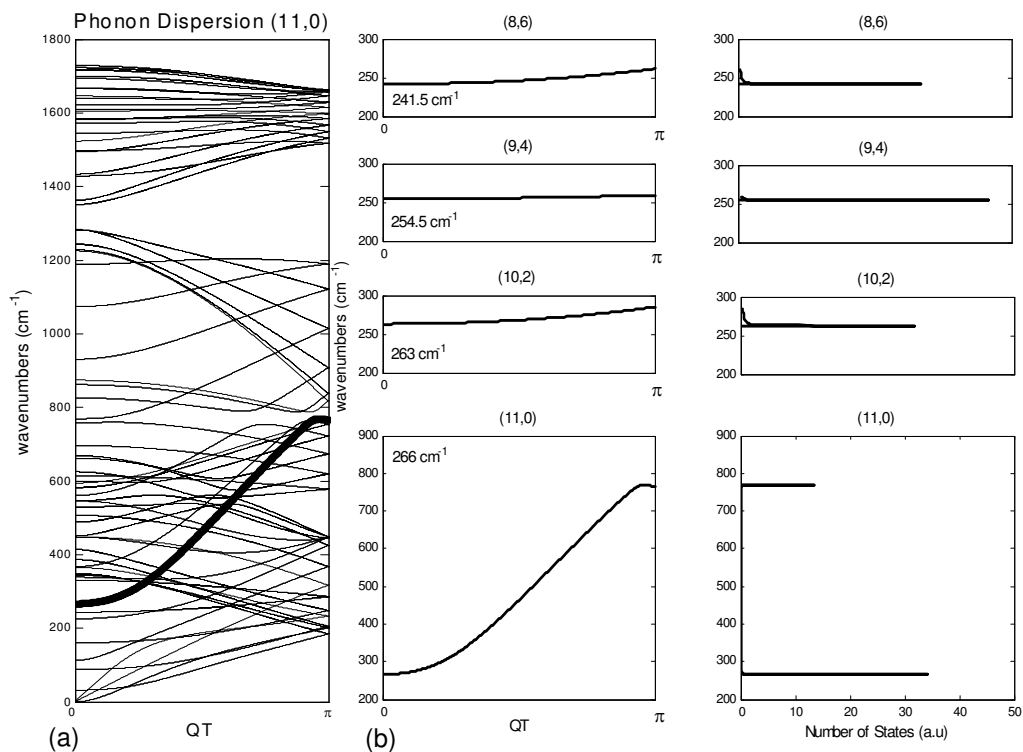


FIG. 1: (a) The phonon dispersion relation for an (11,0) nanotube. The bold line is the RBM dispersion curve. (b) The RBM dispersion and RBM DOS for family 22 SWNTs. The number in the dispersion figures is the zone-center RBM frequency. In all figures, T is the magnitude of the primitive vector along the tube axis.

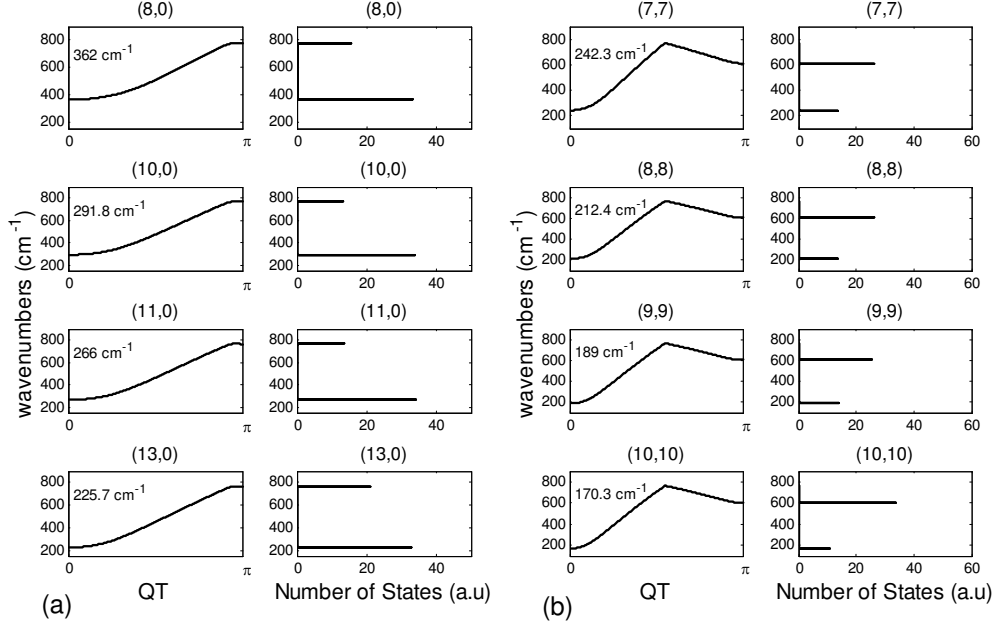


FIG. 2: (a) The RBM dispersion and RBM DOS for zig zag SWNTs (8,0), (10,0), (11,0) and (13,0). (b) The RBM dispersion and RBM DOS for armchair SWNTs (7,7), (8,8), (9,9) and (10,10). The number in the dispersion figures is the zone-center RBM frequency. In all figures, T is the magnitude of the primitive vector along the tube axis.